Fixed-Time Bipartite Consensus of Nonlinear Multi-Agent Systems via Fuzzy Optimization and Quantized Control

Jiaming Guo, Hongjing Liang, and Chenhong An

***Abstract*—In this paper, a fixed-time optimized control scheme with prescribed performance is presented for bipartite consensus of nonlinear multi-agent systems (MASs). To enforce predefined transient and steady-state performance within a fixed time, a fixed-time prescribed performance function (FTPPF) is introduced. The control design is achieved via an identifier-actor-critic framework that approximates the solution to the Hamilton-Jacobi-Bellman equation. Unknown system dynamics are compensated by fuzzy logic systems, and a rounding quantizer processes the signal of the leader to reduce the communication costs. The proposed method ensures all consensus errors converge with prescribed performance bounds in a fixed time. Simulation results validate the theoretical findings.**

***Index Terms*—Fixed-time prescribed performance function (FTPPF), multi-agent systems (MASs), optimal control, bipartite consensus**

I. Introduction

In recent years, because of the significant role of multi-agent systems (MASs) [1] in fields such as artificial intelligence [2] and computer science [3], MASs have garnered extensive research attention. Related technologies with MASs have gained widespread application in many aspects: formation [4], flocking [5], cooperative [6], sensor network [7], and consensus [8, 9]. For the most parts the study of MASs is intimately related to consensus control. When studying the consensus control of MASs, it is often inevitable to address the capacity constraints of communication links. In practical scenarios, the information transmitted between agents is often of limited length. Through this quantization, although it is not possible to exchange the exact true values, values close to the true values can be transmitted, which is referred as quantized consensus [10]. The use of a quantizer can reduce the impact of interference on signals during transmission.

Optimal control has gradually evolved to become an important design concept in modern control theory [11]. It has achieved significant success, particularly in the field of MASs optimal control [12–15]. Optimal control refers to the minimization of the cost function, which represents the balance between desired performance and available resources [16]. For many nonlinear MASs, the core of optimal control lies in solving the Hamilton-Jacobi-Bellman (HJB) equation [17], which is crucial for determining optimal policies. To address nonlinear issues in systems, reinforcement learning (RL) methods have been proposed as a feasible approach to approximate the solution of the HJB equation [18], yielding some meaningful results. Additionally, the update law for the control strategy is based on an RL method derived from the HJB equation. Presently, adaptive backstepping control methods combined with optimal strategies have evolved into a highly effective solution for ensuring the stability of dynamic systems [19, 20]. In Ref. [21], a neural network-based RL algorithm is implemented under the identifier-critic-actor (ICA) architecture, integrating the HJB equation into each subsystem to optimize control performance. However, the aforementioned literatures focus on MASs with cooperative relationships and neglect those with competitive dynamics. The communication between agents is typically represented via a signed graph [22]. Positive signs indicate cooperation among agents, while negative signs denote competition. This means that message passing between an agent and its neighbors includes both cooperation and conflict. Therefore, when designing MASs, it is necessary to consider these potential relationships and develop a control strategy that can manage both cooperative and competitive interactions. When the algorithm accounts for confrontational interactions, agents can achieve a bipartite consensus, agreeing on values but not necessarily on signs [23]. In practical applications [24], such as distributed computing [25] and communication networks [26], bipartite output consensus control plays an important role. Therefore, how to design a suitable and effective optimized bipartite consensus controller for nonlinear MASs has become a hot topic of research.

It should be recognized that the aforementioned consensus control can only ensure error signals converging to a steady state as time approaches infinity, posing limitations in practical applications. To address this issue, finite-time control has been proposed. A finite-time command filter output feedback control method for a class of nonlinear systems has been

Manuscript received: 1 September 2025; revised: 14 October 2025; accepted: 22 October 2025. *(Corresponding author: Hongjing Liang.)*

Citation: J. Guo, H. Liang, and C. An, Fixed-time bipartite consensus of nonlinear multi-agent systems via fuzzy optimization and quantized control, *Int. J. Intell. Control Syst.*, 2025, 30(4), 295–306.

Jiaming Guo, Hongjing Liang, and Chenhong An are with School of Automation Engineering, University of Electronic Science and Technology of China, Chengdu 611731, China (e-mail: 18336132569@163.com; lianghongjing@uestc.edu.cn; anchenhong2023@163.com).

Digital Object Identifier 10.62678/IJICS202512.10231

proposed [27]. However, the convergence time of finite-time control is dependent on the system's initial conditions, so there is a limitation that the initial conditions should not be too far from the steady state to prevent the convergence time from becoming unbounded. Fixed-time control [28] can precisely address this issue. It holds a distinct advantage over finite-time control by ensuring that the settling time is confined within a constant bound, effectively decoupling the convergence time from the initial conditions. In Ref. [29], the fixed-time consensus of nonlinear MASs is studied, ensuring the consensus tracking error to be driven to a small neighborhood around zero within a fixed time. Additionally, Ref. [30] examines the bipartite tracking consensus problem for coopetition MASs. To reduce the convergence time, a control strategy that can effectively address the bipartite tracking consensus problem within a fixed time is designed. However, the fixed-time control strategies reviewed ensure error convergence within a fixed time period. Nonetheless, these strategies do not guarantee transient performance during the convergence process, which may lead to issues such as significant overshoot in the error. This impacts the stability and effectiveness of the achieved convergence. Therefore, Ref. [31] has investigated how to improve the performance of MASs, such as through prescribed performance control [32–34], which usually refers to the requirement to converge the error within a predefined error range. Building on this foundation, more researches have begun to focus on how to solve the bipartite consensus control problem for nonlinear MASs with prescribed performance [35]. It shall be noted that the performance in the aforementioned MASs can be influenced by the choice of the topology and control parameters, making direct analysis quite challenging. To address this issue, Ref. [36] employs the error transformation function (ETF) to introduce a transformed system, and the stability of this new system ensures that the bipartite consensus error achieves the prescribed performance. To reduce the control costs and achieve prescribed performance, further incorporation of cost optimization strategies is necessary to enhance these methods.

(1) Unlike previous works [19–21] that only focus on solving the problem of optimized consensus control in cooperative MASs, an optimized bipartite consensus control protocol is constructed in this paper through ICA framework-based reinforcement learning algorithm, and the optimized bipartite consensus problem in MASs is addressed by the constructed protocol. A rounding quantizer is further incorporated to guarantee lossless signal transmission from leaders to followers when resolving coopetition issues.

(2) To overcome the limitation of conventional prescribed performance control in Refs. [34, 35] that cannot preset convergence time, fixed-time prescribed performance function (FTPPF) is introduced in this work to enhance the system transient performance. The system performance is improved through the proposed FTPPF mechanism by ensuring that tracking errors are confined to predefined bounds within fixed time.

(3) Aiming at unknown dynamic disturbances in nonlinear MAS, we improve the approximation accuracy of fuzzy logic systems (FLSs) through the uniform coverage design of Gaussian basis functions, and combine with ETF to convert bounded errors into unbounded errors, avoiding instability caused by error overrun in traditional compensation methods and ensuring that the closed-loop system is bounded within fixed time.

Notation $\mathbb{R}$, $\mathbb{R}^+$, and $\mathbb{R}^q$ denote the sets of real numbers, positive real numbers, and the q-dimensional Euclidean spaces, respectively. The symbols $\lfloor\cdot\rfloor$ and $\lceil\cdot\rceil$ represent the floor and ceiling functions, respectively. Similarly, $\lceil y_r\rceil$ denotes the ceiling of y_r, which is the smallest integer greater than or equal to y_r.

Remark 1 The core challenges of bipartite consensus for nonlinear MASs can be specifically summarized into three points.

(1) Dual uncertainties of topology and dynamics: Bipartite consensus relies on signed graphs to describe cooperative and competitive relationships, but in practical systems, not only may the topological structure change dynamically, but each agent also has unknown nonlinear dynamics. Traditional linear control methods cannot directly compensate for nonlinear disturbances, which easily leads to error divergence.

(2) Challenge of coordinating fixed-time convergence and performance constraints: Although finitetime control can shorten the convergence time, the convergence bound depends on initial conditions. Traditional PPF can constrain the error range but cannot preset the convergence time, making it difficult to coordinate the two. That is, how to ensure that the error meets the preset bound within fixed time is a key technical bottleneck that needs to be overcome.

(3) Balance between communication efficiency and signal accuracy: There are bandwidth constraints in communication between agents. Although quantized control can reduce the amount of data transmission, quantization errors may damage the sign synchronization of bipartite consensus. It is necessary to design a quantization mechanism to ensure distortion-free signal transmission while reducing communication cost.

II. Problem Formulation and Preliminaries

A. Graph Theory

The MASs comprise N followers and one leader. The communication topology is represented by a signed graph $\mathcal{G} = \{\mathcal{V}, \mathcal{E}, \mathcal{A}\}$, describing information exchange among the N followers. The edge set is $\mathcal{E} \subseteq \mathcal{V} \times \mathcal{V}$, where $\mathcal{V}$ is the node set. The adjacency matrix $\mathcal{A} = [a_{ij}] \in \mathbb{R}^{N\times N}$ has element a_{ij}. For a balanced graph $\mathcal{G}$, $\mathcal{V}_1$ and $\mathcal{V}_2$ satisfy $\mathcal{V}_1 \cap \mathcal{V}_2 = \emptyset$ and $\mathcal{V}_1 \cup \mathcal{V}_2 = \mathcal{V}$. The degree matrix element d_i is the sum of absolute values in row i, expressed as $D = \mathrm{diag}(d_1, d_2, \ldots, d_N)$. Here, $a_{ij} = 0$ indicates that no information flows from agent i to j; $a_{ij} > 0$ refers to cooperative relationship; and $a_{ij} < 0$ refers to competitive relationship. The Laplacian matrix is $L = D - \mathcal{A}$, and $B = \mathrm{diag}(b_1, b_2, \ldots, b_N)$ represents leader-follower interactions ($b_i > 0$ indicates information reception from leader). The diagonal matrix $\beth = (\mu_1, \mu_2, \ldots, \mu_N)$ satisfies $\mu_i = 1$ if $b_i > 0$ and $\mu_i = -1$ if $b_i < 0$.

B. Fuzzy Logic Systems

For the set $\Omega_x \subset \mathbb{R}^q$, this article employs the following form of FLS to approximate

$$f(x) = \mathcal{W}^{*\mathrm{T}}\kappa(x) + \upsilon(x) \tag{1}$$

where $\kappa(x) = [\kappa(x_1), \kappa(x_2), \ldots, \kappa(x_N)]^{\mathrm{T}}$ is basis function. $\upsilon(x)$ represents the approximation error and must satisfy the condition that $\upsilon(x) < \varsigma$, in which ς is an arbitrarily small positive constant. $\mathcal{W}^*$ represents the ideal constant weight vector that is given as $\mathcal{W}^* = \arg\min_{\mathcal{W}\in\mathbb{R}^q}\left\{\sup_{x\in\Omega_x}|F(x) - \omega^{\mathrm{T}}\kappa(x)|\right\}$. Use the Gaussian function as the basis function

$$\kappa_i(x) = \exp\left(\frac{-(x-p_i)^{\mathrm{T}}(x-p_i)}{\eta_i^2}\right),$$

where $i = 1, 2, \ldots, l$, $l \geqslant 2$ represents the FLS node number, p_i and η_i represent the fuzzy rules and width of the Gaussian function.

Remark 2 The design concept of membership functions mainly involves adopting Gaussian functions as basis functions, and their parameter design follows the principle of covering the input space and uniform distribution. First, the number of nodes is selected to be no less than 2, and it is set to 6 in this paper. It is necessary to ensure that the basis functions can cover all possible value ranges of the agent states, and 6 basis functions can uniformly cover this interval. Second, the centers are set using the uniform sampling method, where center points are selected at equal intervals within the value range of the state variables to ensure that the basis functions are uniformly distributed in the input space. Finally, the widths are set to ensure overlapping regions between adjacent basis functions to avoid approximation blind spots.

C. Problem Formulation

The i-th follower in the MASs can be expressed as

$$\begin{cases} \dot{x}_{i,1} = x_{i,2} + f_{i,1}(\bar{x}_{i,1}), \\ \dot{x}_{i,p} = x_{i,p+1} + f_{i,p}(\bar{x}_{i,p}), \\ \dot{x}_{i,n} = u_i + f_{i,n}(\bar{x}_{i,n}), \\ y_i = x_{i,1} \end{cases} \tag{2}$$

where $i = 1, 2, \ldots, N$, $p = 2, 3, \ldots, n-1$, $\bar{x}_{i,p} = [x_{i,1}, x_{i,2}, \ldots, x_{i,p}]^{\mathrm{T}} \in \mathbb{R}^q$ represents the state vector of the i-th subsystem, $u_i \in \mathbb{R}$ represents the control input, and y_i denotes the system output. The nonlinear function $f_{i,p}$ is smooth and unknown.

D. Quantized Reference

To allow followers associated with the leader to receive the quantized signal in real-time, despite lacking prior knowledge of the leader's reference signal y_r, a quantizer is designed as

$$y_q = cQ(\hat{y}_r(t)),\ \hat{y}_r(t) = \frac{y_r}{c} \tag{3}$$

where $Q(\cdot)$ represents the quantizer, y_r represents the leader's reference signal, and c is a parameter that will be designed later in the process. In this way, the follower can only receive the quantized signal y_q. Here, a rounding quantizer is chosen, the rounding quantizer Q has the property of rounding real numbers to the nearest integer, so the form of the received signal y_q is

$$y_q = 2\begin{cases} c\lfloor\hat{y}_r\rfloor,\ \hat{y}_r - \lfloor\hat{y}_r\rfloor < \dfrac{1}{2}; \\ c\lceil\hat{y}_r\rceil,\ \hat{y}_r - \lceil\hat{y}_r\rceil \geqslant \dfrac{1}{2} \end{cases} \tag{4}$$

Remark 3 This quantizer rounds the quantized leader reference signal to the nearest integer, so the upper bound of the error is directly determined by c. The relationship between the quantizer parameter c and communication cost is reflected through the accuracy-cost tradeoff. (1) Increasing c reduces communication costs but compromises accuracy. As c increases, the number of quantization levels decreases, resulting in less data transmitted per unit time; however, when the upper bound of the quantization error increases, it may affect the sign synchronization of bipartite consensus. (2) When c decreases, the number of quantization levels increases, the upper bound of the error decreases, which can ensure the accuracy of signal transmission, but the communication cost increases.

E. Transformation of Error

In order to confine the virtual error within the prescribed performance region, ETF and FTPPF are introduced. The FTPPF is denoted by the symbol $\nu_{i,p}(t)$, and $\nu_{i,p}(t)$ can be expressed in the following form

$$\nu_{i,p}(t) = \begin{cases} (\nu_{i,p,0}^{k_{i,p}} - k_{i,p}\delta_{i,p}t)^{1/k_{i,p}},\ 0 \leqslant t < \tilde{\Upsilon}_{i,p}; \\ \nu_{\tilde{\Upsilon}_{i,p}},\ t \geqslant \tilde{\Upsilon}_{i,p} \end{cases} \tag{5}$$

where $\nu_{i,p,0}$, $k_{i,p}$, $\delta_{i,p}$, and $\nu_{\tilde{\Upsilon}_{i,p}}$ are positive parameters that need to be designed. Additionally, it requires special attention that $o_{i,p} \geqslant \kappa_{i,p}$, $o_{i,p} = 2N$, and $\kappa_{i,p} = 2M+1$, and N and M both are natural numbers. It needs to be specified that the settling time is denoted by $\tilde{\Upsilon}_{i,p} = \nu_{i,p,0}^{k_{i,p}}/(k_{i,p}\delta_{i,p})$, where the initial error boundary is defined as $\nu_{i,p}(0) = \nu_{i,p,0}$. Furthermore, the corresponding steady-state error boundary is given by $\nu_{\tilde{\Upsilon}_{i,p}} = \lim_{t\to\tilde{\Upsilon}_{i,p}} \nu_{i,p}(t)$.

Remark 4 When the function $\nu_{i,p}(t)$ is chosen as the FTPPF, the conditions that $\nu_{i,p}(t)$ needs to satisfy are as follows. (1) $\nu_{i,p}(t)$ is a function that is always positive and meets the condition of being monotonically decreasing. (2) For any given arbitrarily small positive real number $\tilde{\Upsilon}_{i,p}$, $\lim_{t\to\tilde{\Upsilon}_{i,p}} \nu_{i,p}(t) = \nu_{\tilde{\Upsilon}_{i,p}}$ holds. (3) For any arbitrary $t \geqslant \tilde{\Upsilon}_{i,p}$, $\nu_{i,p}(t) = \nu_{\tilde{\Upsilon}_{i,p}}$ holds.

Remark 5 The FTPPF proposed in this paper achieves improvements through piecewise design and adjustable parameters. First, through piecewise function design, the function decreases monotonically before reaching the fixed settling time, where the settling time can be directly preset via the initial bound, decay order, and decay rate, solving the "uncontrollable convergence time" problem of traditional PPF. Second, after reaching the fixed settling time, the function provides a steady-state bound, the upper limit of the steady-state error can be set according to requirements, and the decay order can be flexibly selected, specifically, when the initial error is large, $k_{i,p}$ can be increased to accelerate decay and avoid overshoot.

The ETF used here is $\Lambda_{i,m}(\varrho_{i,m}(t))$ for $m=\{1,2,\ldots,n-1\}$, the ETF is chosen to be

$$\Lambda_{i,m}(\varrho_{i,m}(t))=\frac{2}{\pi}\arctan(\varrho_{i,m}(t)) \tag{6}$$

In addition, $e_{i,m}$ can be defined as

$$e_{i,m}=\nu_{i,m}(t)\Lambda_{i,m}(\varrho_{i,m}(t)) \tag{7}$$

Remark 6 From the above, it is known that the relationship between the transformed error and the consistent error can be expressed as $\varrho_{i,m}(t)=\tan\dfrac{\pi e_{i,m}(t)}{2\nu_{i,m}(t)}$. Incorporating inequalities $\nu_{i,m}(t)>0$ and $-1<\Lambda_{i,m}(\varrho_{i,m}(t))<1$, then inequality $-\nu_{i,m}(t)<e_{i,m}=\nu_{i,m}(t)\Lambda_{i,m}(\varrho_{i,m}(t))<\nu_{i,m}(t)$ is derived. $\Lambda_{i,m}(\varrho_{i,m}(t))$ has the following properties. (1) $\Lambda_{i,m}(\varrho_{i,m}(t))$ is a smooth function and has the property of being strictly monotonically increasing. (2) The range of values for $\Lambda_{i,m}(\varrho_{i,m}(t))$ is $\Lambda_{i,m}(\varrho_{i,m}(t))\in(-1,1)$, where $\varrho_{i,m}(t)$ is the transformed error. (3) The limiting cases for the values of $\Lambda_{i,m}(\varrho_{i,m}(t))$ are $\lim\limits_{\varrho_{i,m}(t)\to\infty}\Lambda_{i,m}(\varrho_{i,m}(t))=-1$ and $\lim\limits_{\varrho_{i,m}(t)\to\infty}\Lambda_{i,m}(\varrho_{i,m}(t))=1$.

III. Optimal Controller Design

In this section, we incorporate an ICA framework to design a fuzzy optimization consensus control protocol based on RL. The consistent error of the quantized MASs studied in this article is represented by

$$e_{i,1}=\sum_{p\in N_i}|a_{i,p}|(y_i-y_p)+b_i(y_i-\mu_i y_q) \tag{8}$$

The expression for other errors is as follows

$$e_{i,p}=x_{i,p}-\alpha_{i,p-1},\ p\in 2,3,\ldots,n \tag{9}$$

Taking the derivative of Eq. (8) to Eq. (10) with respect to time yields

$$\begin{aligned}\dot e_{i,1}&=(d_i+b_i)\dot x_{i,1}-\sum_{j\in N_i}|a_{i,j}|\dot x_{j,1}-b_i\mu_i\dot y_q=\\&(d_i+b_i)(f_{i,1}(\bar x_{i,1})+x_{i,2})-\sum_{j\in N_i}|a_{i,j}|(x_{j,2}+\\&f_{j,1}(\bar x_{j,1}))-b_i\mu_i\dot y_q\end{aligned} \tag{10}$$

$$\dot e_{i,p}=\dot x_{i,p}-\dot\alpha_{i,p-1}=f_{i,p}(\bar x_{i,p})+x_{i,p+1}-\dot\alpha_{i,p-1} \tag{11}$$

$$\dot e_{i,n}=\dot x_{i,n}-\dot\alpha_{i,n-1}=f_{i,n}(\bar x_{i,n})+u_i-\dot\alpha_{i,n-1} \tag{12}$$

Combining Eq. (7) $e_{i,m}$ can be expressed in the following form

$$\begin{aligned}\dot e_{i,m}=\nu_{i,m}(t)\frac{\partial\Lambda_{i,m}(\varrho_{i,m}(t))}{\partial\varrho_{i,m}(t)}\dot\varrho_{i,m}(t)+\\\dot\nu_{i,m}(t)\Lambda_{i,m}(\varrho_{i,m}(t))\end{aligned} \tag{13}$$

To simplify the equations, $\varpi_{i,p}$ and $\psi_{i,p}$ are defined as

$$\varpi_{i,p}(\varrho_{i,p}(t),\nu_{i,p}(t))=-\frac{\dot\nu_{i,p}(t)\Lambda_{i,p}(\varrho_{i,p}(t))}{\nu_{i,p}(t)\dfrac{\partial\Lambda_{i,p}(\varrho_{i,p}(t))}{\partial\varrho_{i,p}(t)}},$$

$$\psi_{i,p}(\varrho_{i,p}(t),\nu_{i,p}(t))=-\frac{1}{\nu_{i,p}(t)\dfrac{\partial\Lambda_{i,p}(\varrho_{i,p}(t))}{\partial\varrho_{i,p}(t)}}.$$

Furthermore, the dynamical equation for the transformed error results in

$$\begin{aligned}\dot\varrho_{i,1}=\varpi_{i,1}+\psi_{i,1}\Big[(d_i+b_i)(x_{i,2}+f_{i,1}(\bar x_{i,1}))-\\\sum_{j\in N_i}|a_{i,j}|(x_{j,2}+f_{j,1}(x_{j,1}))-b_i\mu_i\dot y_q\Big]\end{aligned} \tag{14}$$

$$\dot\varrho_{i,p}=\varpi_{i,p}+\psi_{i,p}(x_{i,p+1}+f_{i,p}(\bar x_{i,p})-\dot\alpha_{i,p-1}) \tag{15}$$

$$\dot\varrho_{i,n}=\varpi_{i,n}+\psi_{i,n}(u_i+f_{i,n}(\bar x_{i,n})-\dot\alpha_{i,n-1}) \tag{16}$$

Step 1 Design the value function $\beta_{i,1}=\varrho_{i,1}^2+\alpha_{i,1}^2$ and establish the optimal value function as

$$J_{i,1}^*(\varrho_{i,1}(t))=\min_{\alpha_1\in\Omega_x}\int_0^\infty(\varrho_{i,1}^2(t)+\alpha_{i,1}^2(t))\mathrm{d}t \tag{17}$$

where Ω_x is the set of all allowable control inputs and α_1 is the virtual control.

Thus, the HJB equation is

$$H_{i,1}\left(\varrho_{i,1},\alpha_{i,1}^*,\frac{\partial J_{i,1}^*}{\partial\varrho_{i,1}}\right)=\varrho_{i,1}^2+\alpha_{i,1}^{*2}+\frac{\partial J_{i,1}^*}{\partial\varrho_{i,1}}\dot\varrho_{i,1}=0 \tag{18}$$

By processing $\dfrac{\partial H_{i,1}}{\partial\alpha_{i,1}^*}=0$, the optimal virtual controller $\alpha_{i,1}^*$ can be obtained.

$$\alpha_{i,1}^*=-\frac{\vartheta_{i,1}}{2}\frac{\partial J_{i,1}^*}{\partial\varrho_{i,1}} \tag{19}$$

where $\vartheta_{i,1}=\psi_{i,1}(d_i+b_i)$.

To achieve consensus tracking control, $\dfrac{\partial J_{i,1}^*}{\partial\varrho_{i,1}}$ can be decomposed into the following formula

$$\frac{\partial J_{i,1}^*}{\partial\varrho_{i,1}}=\frac{1}{\vartheta_{i,1}^2}(2\tau_{i,1}\varrho_{i,1}+2F_{i,1}+J_{i,1}^0) \tag{20}$$

where $J_{i,1}^0=\vartheta_{i,1}^2\dfrac{\partial J_{i,1}^*}{\partial\varrho_{i,1}}-2\tau_{i,1}\varrho_{i,1}-2F_{i,1}$, $F_{i,1}=\psi_{i,1}[(d_i+b_i)(f_{i,1}(\bar x_{i,1})+x_{i,2})-\sum_{j\in N_i}|a_{i,j}|(x_{j,2}+f_{j,1}(\bar x_{j,1}))+\psi_{i,1}^{-1}\varpi_{i,1}-b_i\mu_i\dot y_q]+\varrho_{i,1}$, and $\tau_{i,1}>1$ is a parameter that will be designed later in the process.

Combining Eqs. (20) and (21), the optimal form of the virtual controller can be obtained.

$$\alpha_{i,1}^*=\frac{1}{\vartheta_{i,1}}(-\tau_{i,1}\varrho_{i,1}-F_{i,1}+J_{i,1}^0) \tag{21}$$

The following expression can be derived by approximating $F_{i,1}$ and $J_{i,1}^0$ via FLS.

$$F_{i,1}=W_{fi,1}^{\mathrm T}S_{fi,1}+\phi_{fi,1} \tag{22}$$

$$J_{i,1}^0=W_{i,1}^{\mathrm T}S_{i,1}+\phi_{i,1} \tag{23}$$

Substituting Eq. (23) into Eqs. (21) and (22), we have

$$\begin{aligned}\frac{\partial J_{i,1}^*}{\partial\varrho_{i,1}}=\frac{1}{\vartheta_{i,1}^2}(2\tau_{i,1}\varrho_{i,1}+2W_{fi,1}^{\mathrm T}S_{fi,1}+\\2\phi_{fi,1}+\phi_{i,1}+W_{i,1}^{\mathrm T}S_{i,1})\end{aligned} \tag{24}$$

$$\alpha_{i,1}^* = \frac{1}{\vartheta_{i,1}}(-\tau_{i,1}\varrho_{i,1} - W_{fi,1}^{\mathrm{T}}S_{fi,1} - \phi_{fi,1} - \frac{1}{2}\phi_{i,1} - \frac{1}{2}W_{i,1}^{\mathrm{T}}S_{i,1}) \tag{25}$$

Because of the presence of unknown terms $\phi_{fi,1}$ and $\phi_{i,1}$ in Eqs. (25) and (26), an RL based ICA framework is proposed to develop a virtually usable controller. This framework is engineered to tackle the challenges inherent to the virtual controllers that incorporate the virtual control elements, which may not be directly applicable. By harnessing the ICA framework within RL, the system is enabled to adaptively learn and refine its control strategy, thereby ensuring the efficient application of the virtual controller.

First, an identifier is used to identify $F_{i,1}$

$$\hat{F}_{i,1} = \hat{W}_{fi,1}^{\mathrm{T}}S_{fi,1} \tag{26}$$

where $\hat{F}_{i,1}$ is the identifier output and $\hat{W}_{fi,1}$ is the identifier fuzzy parameter vector.

The identifier FLS parameter vector $\hat{W}_{fi,1}$ is updated by the following law

$$\dot{\hat{W}}_{fi,1} = \wp_{fi,1}(\psi_{i,1}S_{fi,1}\varrho_{i,1} - \rho_{fi,1}\hat{W}_{fi,1}) \tag{27}$$

where $\wp_{fi,1} > 0$ and $\rho_{fi,1} > 0$ are parameters that need to be designed later in the process.

Combining Eq. (25), we design the critic expression that evaluates the control performance

$$\frac{\partial \hat{J}_{i,1}^*}{\partial \varrho_{i,1}} = \frac{1}{\vartheta_{i,1}^2}(2\tau_{i,1}\varrho_{i,1} + 2W_{fi,1}^{\mathrm{T}}S_{fi,1} + W_{ci,1}^{\mathrm{T}}S_{i,1}) \tag{28}$$

Similar to $F_{i,1}$, $\dfrac{\partial \hat{J}_{i,1}^*}{\partial \varrho_{i,1}}$ is the estimate of $\dfrac{\partial J_{i,1}^*}{\partial \varrho_{i,1}}$. It should be noted that $\hat{W}_{ci,1}$ is the critic fuzzy parameter vector and its update law is

$$\dot{\hat{W}}_{ci,1} = -\wp_{ci,1}S_{Ri,1}S_{Ri,1}^{\mathrm{T}}\hat{W}_{ci,1} \tag{29}$$

where $\wp_{ci,1}$ is a positive parameter that needs to be designed later in the process.

Based on Eq. (26), the actor responsible for carrying out control actions is designed in the following manner

$$\hat{\alpha}_{i,1}^* = \frac{1}{\vartheta_{i,1}}\left(-\tau_{i,1}\varrho_{i,1} - W_{fi,1}^{\mathrm{T}}S_{fi,1} - \frac{1}{2}W_{ai,1}^{\mathrm{T}}S_{i,1}\right) \tag{30}$$

where $\hat{\alpha}_{i,1}^*$ is the estimate of $\alpha_{i,1}^*$.

It should be noted that $\hat{W}_{ai,1}$ is the actor FLS parameter vector and its update law is

$$\dot{\hat{W}}_{ai,1} = -S_{Ri,1}S_{Ri,1}^{\mathrm{T}}(\wp_{ai,1}(\hat{W}_{ai,1} - \hat{W}_{ci,1}) + \wp_{ci,1}\hat{W}_{ci,1}) \tag{31}$$

where $\wp_{ai,1}$ is a positive parameter that needs to be designed later in the process and it is necessary to meet the conditions: $\wp_{ai,1} > 0$, $\wp_{ci,1} > 0.5$, and $\wp_{ci,1} > \wp_{ai,1}/2$.

Step *p* Establish the optimal value function

$$J_{i,p}^*(\varrho_{i,p}(t)) = \min_{\alpha_p \in \Omega_x}\int_0^{\infty}(\varrho_{i,p}^2(t) + \alpha_{i,p}^2(t))\mathrm{d}t \tag{32}$$

Thus, the HJB equation is

$$H_{i,p}\left(\varrho_{i,p}, \alpha_{i,p}^*, \frac{\partial J_{i,p}^*}{\partial \varrho_{i,p}}\right) = \varrho_{i,p}^2 + \alpha_{i,p}^{*2} + \frac{\partial J_{i,p}^*}{\partial \varrho_{i,p}}\dot{\varrho}_{i,p} = 0 \tag{33}$$

where $\alpha_{i,p}^*$ represents the virtual control strategy that minimizes $\varrho_{i,p}^2 + \alpha_{i,p}^{*2}$.

Similar to Eq. (20), the optimal virtual controller $\alpha_{i,p}^*$ can be obtained.

$$\alpha_{i,p}^* = -\frac{\psi_{i,p}}{2}\frac{\partial J_{i,p}^*}{\partial \varrho_{i,p}} \tag{34}$$

$\dfrac{\partial J_{i,p}^*}{\partial \varrho_{i,p}}$ can be decomposed into the following formula

$$\frac{\partial J_{i,p}^*}{\partial \varrho_{i,p}} = \frac{1}{\psi_{i,p}^2}(2\tau_{i,p}\varrho_{i,p} + 2F_{i,p} + J_{i,p}^0) \tag{35}$$

where $J_{i,p}^0 = \psi_{i,p}^2\dfrac{\partial J_{i,p}^*}{\partial \varrho_{i,p}} - 2\tau_{i,p}\varrho_{i,p} - 2F_{i,p}$ and $F_{i,p} = \psi_{i,p}[x_{i,p+1} + f_{i,p}(\bar{x}_{i,p}) - \dot{\alpha}_{i,p-1}] + \varrho_{i,p}$, $\tau_{i,p} > 1$ is a parameter that will be designed later in the process.

Combining Eqs. (35) and (36), the optimal form of the virtual controller can be obtained

$$\alpha_{i,p}^* = \frac{1}{\psi_{i,p}}(-\tau_{i,p}\varrho_{i,p} - F_{i,p} + J_{i,p}^0) \tag{36}$$

Using FLS to approximate $F_{i,p}$ and $J_{i,p}^0$, we can derive the following expressions

$$F_{i,p} = W_{fi,p}^{\mathrm{T}}S_{fi,p} + \phi_{fi,p} \tag{37}$$

$$J_{i,p}^0 = W_{i,p}^{\mathrm{T}}S_{i,p} + \phi_{i,p} \tag{38}$$

Substituting Eq. (38) into Eqs. (36) and (37) sequentially, we get

$$\frac{\partial J_{i,p}^*}{\partial \varrho_{i,p}} = \frac{1}{\psi_{i,p}^2}(2\tau_{i,p}\varrho_{i,p} + 2W_{fi,p}^{\mathrm{T}}S_{fi,p} + 2\phi_{fi,p} + \phi_{i,p} + W_{i,p}^{\mathrm{T}}S_{i,p}) \tag{39}$$

$$\alpha_{i,p}^* = \frac{1}{\psi_{i,p}}(-\tau_{i,p}\varrho_{i,p} - W_{fi,p}^{\mathrm{T}}S_{fi,p} - \phi_{fi,p} - \frac{1}{2}\phi_{i,p} - \frac{1}{2}W_{i,p}^{\mathrm{T}}S_{i,p}) \tag{40}$$

Similar to Eq. (27), an identifier is used to identify $F_{i,p}$

$$\hat{F}_{i,p} = \hat{W}_{fi,p}^{\mathrm{T}}S_{fi,p} \tag{41}$$

where $\hat{F}_{i,p}$ is the identifier output, and $\hat{W}_{fi,p}$ is the identifier fuzzy parameter vector.

The identifier FLS parameter vector $\hat{W}_{fi,p}$ is updated by the following law

$$\dot{\hat{W}}_{fi,p} = \wp_{fi,p}(\psi_{i,p}S_{fi,p}\varrho_{i,p} - \rho_{fi,p}\hat{W}_{fi,p}) \tag{42}$$

where $\wp_{fi,p} > 0$ and $\rho_{fi,p} > 0$ are parameters that need to be designed later in the process.

Combining Eq. (40), we design the critic expression that evaluates the control performance

$$\frac{\partial \hat{J}_{i,p}^*}{\partial \varrho_{i,p}} = \frac{1}{\psi_{i,p}^2}(2\tau_{i,p}\varrho_{i,p} + 2W_{fi,p}^{\mathrm{T}}S_{fi,p} + W_{ci,p}^{\mathrm{T}}S_{i,p}) \tag{43}$$

Similar to $F_{i,p}$, where $\frac{\partial \hat{J}_{i,p}^*}{\partial \varrho_{i,p}}$ is the estimate of $\frac{\partial J_{i,p}^*}{\partial \varrho_{i,p}}$. It shall be noted that $\hat{W}_{ci,p}$ is the critic fuzzy parameter vector, and its update law is

$$\dot{\hat{W}}_{ci,p} = -\wp_{ci,p} S_{Ri,p} S_{Ri,p}^{\mathrm{T}} \hat{W}_{ci,p} \tag{44}$$

where $\wp_{ci,p}$ is a positive parameter that needs to be designed later in the process.

Based on Eq. (41), the actor responsible for carrying out control actions is designed in the following manner

$$\hat{\alpha}_{i,p}^* = \frac{1}{\psi_{i,p}} \left(-\tau_{i,p}\varrho_{i,p} - W_{fi,p}^{\mathrm{T}} S_{fi,p} - \frac{1}{2} W_{ai,p}^{\mathrm{T}} S_{i,p} \right) \tag{45}$$

Similar to $F_{i,p}$, where $\hat{\alpha}_{i,p}^*$ is the estimate of $\alpha_{i,p}^*$. It shall be noted that $\hat{W}_{ai,p}$ is the actor FLS parameter vector, and its update law is

$$\dot{\hat{W}}_{ai,p} = -S_{Ri,p} S_{Ri,p}^{\mathrm{T}} (\wp_{ai,p}(\hat{W}_{ai,p} - \hat{W}_{ci,p}) + \wp_{ci,p} \hat{W}_{ci,p}) \tag{46}$$

where $\wp_{ai,p}$ is a positive parameter that needs to be designed later in the process, and it is necessary to meet the conditions: $\wp_{ai,p} > 0$, $\wp_{ci,p} > 0.5$, and $\wp_{ci,p} > \wp_{ai,p}/2$.

Step *n* Design the optimal value function

$$J_{i,n}^*(\varrho_{i,n}(t)) = \min_{u_i \in \Omega_x} \int_0^\infty (\varrho_{i,n}^2(t) + u_i^2(t)) \mathrm{d}t \tag{47}$$

Thus, the HJB equation is

$$H_{i,n}\left(\varrho_{i,n}, u_i^*, \frac{\partial J_{i,n}^*}{\partial \varrho_{i,n}} \right) = \varrho_{i,n}^2 + u_i^{*2} + \frac{\partial J_{i,n}^*}{\partial \varrho_{i,n}} \dot{\varrho}_{i,n} = 0 \tag{48}$$

where u_i^* represents the control strategy that has the minimum value of $\varrho_{i,n}^2 + u_i^{*2}$.

The optimal controller u_i^* can be obtained

$$u_i^* = -\frac{\psi_{i,n}}{2} \frac{\partial J_{i,n}^*}{\partial \varrho_{i,n}} \tag{49}$$

$\frac{\partial J_{i,n}^*}{\partial \varrho_{i,n}}$ can be decomposed into the following formula

$$\frac{\partial J_{i,n}^*}{\partial \varrho_{i,n}} = \frac{1}{\psi_{i,n}^2} (2\tau_{i,n}\varrho_{i,n} + 2F_{i,n} + J_{i,n}^0) \tag{50}$$

where $J_{i,n}^0 = \psi_{i,n}^2 \frac{\partial J_{i,n}^*}{\partial \varrho_{i,n}} - 2\tau_{i,n}\varrho_{i,n} - 2F_{i,n}$, $F_{i,n} = \psi_{i,n}[u_i + f_{i,n}(\bar{x}_{i,n}) - \dot{\alpha}_{i,n-1}] + \varrho_{i,n}$, and $\tau_{i,n} > 1$ are parameters that will be designed later in the process.

The optimal form of the controller can be obtained

$$u_i^* = \frac{1}{\psi_{i,n}} (-\tau_{i,n}\varrho_{i,n} - F_{i,n} + J_{i,n}^0) \tag{51}$$

Using FLS to approximate $F_{i,n}$ and $J_{i,n}^0$, we have

$$F_{i,n} = W_{fi,n}^{\mathrm{T}} S_{fi,n} + \phi_{fi,n} \tag{52}$$

$$J_{i,n}^0 = W_{i,n}^{\mathrm{T}} S_{i,n} + \phi_{i,n} \tag{53}$$

By substituting Eq. (53) into Eqs. (51) and (52) sequentially, the following results are obtained

$$\begin{aligned} \frac{\partial J_{i,n}^*}{\partial \varrho_{i,n}} = \frac{1}{\psi_{i,n}^2} (2\tau_{i,n}\varrho_{i,n} + 2W_{fi,n}^{\mathrm{T}} S_{fi,n} + 2\phi_{fi,n} + \\ \phi_{i,n} + W_{i,n}^{\mathrm{T}} S_{i,n}) \end{aligned} \tag{54}$$

$$\begin{aligned} u_i^* = \frac{1}{\psi_{i,n}} (-\tau_{i,n}\varrho_{i,n} - W_{fi,n}^{\mathrm{T}} S_{fi,n} - \phi_{fi,n} - \\ \frac{1}{2}\phi_{i,n} - \frac{1}{2} W_{i,n}^{\mathrm{T}} S_{i,n}) \end{aligned} \tag{55}$$

Using the identifier to identify $F_{i,n}$ yields

$$\hat{F}_{i,n} = \hat{W}_{fi,n}^{\mathrm{T}} S_{fi,n} \tag{56}$$

where $\hat{F}_{i,n}$ is the identifier output and $\hat{W}_{fi,n}$ is the identifier fuzzy parameter vector.

$\hat{W}_{fi,n}$ is updated by the following law

$$\dot{\hat{W}}_{fi,n} = \wp_{fi,n}(\psi_{i,n} S_{fi,n}\varrho_{i,n} - \rho_{fi,n} \hat{W}_{fi,n}) \tag{57}$$

where $\wp_{fi,n} > 0$ and $\rho_{fi,n} > 0$ need to be designed later, and all of them are positive numbers.

Combining Eq. (55), we design the critic expression that evaluates the control performance

$$\frac{\partial \hat{J}_{i,n}^*}{\partial \varrho_{i,n}} = \frac{1}{\psi_{i,n}^2} (2\tau_{i,n}\varrho_{i,n} + 2W_{fi,n}^{\mathrm{T}} S_{fi,n} + W_{ci,n}^{\mathrm{T}} S_{i,n}) \tag{58}$$

$\hat{W}_{ci,n}$ is the critic fuzzy parameter vector, and its update law is

$$\dot{\hat{W}}_{ci,n} = -\wp_{ci,n} S_{Ri,n} S_{Ri,n}^{\mathrm{T}} \hat{W}_{ci,n} \tag{59}$$

where $\wp_{ci,n}$ is a positive parameter.

Based on Eq. (56), the actor responsible for carrying out control actions is designed in the following manner

$$\hat{u}_i^* = \frac{1}{\psi_{i,n}} \left(-\tau_{i,n}\varrho_{i,n} - W_{fi,n}^{\mathrm{T}} S_{fi,n} - \frac{1}{2} W_{ai,n}^{\mathrm{T}} S_{i,n} \right) \tag{60}$$

The actor FLS parameter vector, which is denoted by $\hat{W}_{ai,n}$, is updated according to the following law

$$\dot{\hat{W}}_{ai,n} = -S_{Ri,n} S_{Ri,n}^{\mathrm{T}} (\wp_{ai,n}(\hat{W}_{ai,n} - \hat{W}_{ci,n}) + \wp_{ci,n} \hat{W}_{ci,n}) \tag{61}$$

where $\wp_{ai,n}$ is a positive parameter that needs to be designed later, and it is necessary to meet the conditions: $\wp_{ai,n} > 0$, $\wp_{ci,n} > 0.5$, and $\wp_{ci,n} > \wp_{ai,n}/2$.

Remark 7 This paper adapts the ICA framework to fixed time control requirements through update law gain design and error feedback correction. First, the identifier is used to approximate unknown terms, and an error transformation coefficient related to the FTPPF is introduced into its update law to ensure that the convergence rate of the identifier matches the decay rate of the FTPPF, avoiding error overrun caused by lag in unknown term compensation. Second, the critic evaluates control performance by estimating the derivative of the optimal value function, and the critic gain in its update law must satisfy specific conditions to ensure that the value function converges to the optimal value within fixed time and provides accurate performance feedback for the actor. Finally, the actor designs the control law based on feedback from the critic, an actor gain is introduced into its update law, and this actor gain must meet specific constraint conditions. These constraints ensure that the adjustment rate of the actor's output is greater than the error growth rate, thereby guaranteeing that the error converges within the preset fixed time.

IV. Stability Analysis

Theorem 1 By following the control protocol established according to the aforementioned formulas, the identifier, critic, and actor are updated respectively via the corresponding update laws. The identifier is updated by the laws in Eqs. (27), (42), and (57) corresponding to Eqs. (28), (43), and (58); the critic is updated by the laws in Eqs. (29), (44), and (59) corresponding to Eqs. (30), (45), and (60); and the actor is updated by the laws in Eqs. (31), (46), and (61) corresponding to Eqs. (32), (47), and (62), respectively. Under this control protocol, the bipartite consensus error converges within a fixed time and satisfies the prescribed performance control objectives. Additionally, it should be specifically noted that all closed-loop signals of the system described in Eq. (2) are bounded.

Proof The main content of the proof is stability analysis.

Step 1 Choose the Lyapunov function as

$$V_{i,1}=\sum_{i=1}^{N}\left(\frac{1}{2}\varrho_{i,1}^2+\frac{1}{2\wp_{fi,1}}\tilde{W}_{fi,1}^{\mathrm{T}}\tilde{W}_{fi,1}+\frac{1}{2}\sum_{h=a,c}\tilde{W}_{hi,1}^{\mathrm{T}}\tilde{W}_{hi,1}\right) \tag{62}$$

where $\tilde{W}(\cdot)=\hat{W}(\cdot)-W(\cdot)$, and since $W(\cdot)$ is a constant, it follows that $\dot{\tilde{W}}(\cdot)=\dot{\hat{W}}(\cdot)$.

The derivative of $V_{i,1}$ can be expressed as

$$\begin{aligned}\dot{V}_{i,1}=&\sum_{i=1}^{N}\varrho_{i,1}\Bigg\{\psi_{i,1}\Bigg((d_i+b_i)(\varrho_{i,2}+\alpha_{i,1}+f_{i,1}(\bar{x}_{i,1}))+\\&\varpi_{i,1}\psi_{i,1}^{-1}-\sum_{j\in N_i}|a_{i,j}|(x_{j,2}+f_{j,1}(x_{j,1}))\Bigg)-b_i\mu_i\dot{y}_q\Bigg\}+\\&\sum_{i=1}^{N}\left\{\frac{1}{\wp_{fi,1}}\tilde{W}_{fi,1}^{\mathrm{T}}\wp_{fi,1}(\psi_{i,1}S_{fi,1}\varrho_{i,1}-\rho_{fi,1}\hat{W}_{fi,1})\right\}-\\&\sum_{i=1}^{N}\{\tilde{W}_{ai,1}^{\mathrm{T}}S_{Ri,1}S_{Ri,1}^{\mathrm{T}}(\wp_{ai,1}(\hat{W}_{ai,1}-\hat{W}_{ci,1})+\\&\wp_{ci,1}\hat{W}_{ci,1})\}-\sum_{i=1}^{N}\{\wp_{ci,1}\tilde{W}_{ci,1}S_{Ri,1}S_{Ri,1}^{\mathrm{T}}\hat{W}_{ci,1}\}\end{aligned} \tag{63}$$

Applying the Young's inequality, we have

$$\begin{aligned}&\sum_{i=1}^{N}\zeta_{i,1}e_{i,2}\leqslant\sum_{i=1}^{N}\frac{\varrho_{i,1}^2}{2}+\sum_{i=1}^{N}\frac{\vartheta_{i,1}^2e_{i,2}^2}{2},\\&\sum_{i=1}^{N}\wp_{ci,1}\tilde{W}_{ai,1}^{\mathrm{T}}S_{Ri,1}S_{Ri,1}^{\mathrm{T}}\hat{W}_{ci,1}\leqslant\\&\sum_{i=1}^{N}\frac{\wp_{ci,1}(\tilde{W}_{ai,1}^{\mathrm{T}}S_{Ri,1})^2}{2}+\sum_{i=1}^{N}\frac{\wp_{ci,1}(\hat{W}_{ci,1}S_{Ri,1}^{\mathrm{T}})^2}{2},\\&\sum_{i=1}^{N}\left(-\frac{1}{2\vartheta_{i,1}}\zeta_{i,1}\hat{W}_{ai,1}^{\mathrm{T}}S_{Ri,1}\right)\leqslant\\&\sum_{i=1}^{N}\frac{\varrho_{i,1}^2}{4}+\sum_{i=1}^{N}\frac{(\hat{W}_{ai,1}^{\mathrm{T}}S_{Ri,1})^2}{4}\end{aligned} \tag{64}$$

where $\zeta_{i,1}=\varrho_{i,1}\psi_{i,1}(d_i+b_i)$.

Additionally, we can handle the remaining terms by deducing the following equation

$$\begin{aligned}&\tilde{W}^{\mathrm{T}}(\cdot)\hat{W}(\cdot)=\\&\frac{1}{2}(\tilde{W}^{\mathrm{T}}(\cdot)\tilde{W}(\cdot)+\hat{W}^{\mathrm{T}}(\cdot)\hat{W}(\cdot)-W^{\mathrm{T}}(\cdot)W(\cdot))\end{aligned} \tag{65}$$

By organizing all the previous reasoning results, we obtain

$$\begin{aligned}\dot{V}_{i,1}\leqslant&\sum_{i=1}^{N}\frac{\vartheta_{i,1}^2}{2}e_{i,2}^2-\sum_{i=1}^{N}\left(\frac{\tau_{i,1}}{2}-\frac{1}{4}\right)\varrho_{i,1}^2+\Gamma_{i,1}-\\&\sum_{i=1}^{N}\frac{\rho_{fi,1}}{2}W_{fi,1}^{\mathrm{T}}W_{fi,1}-\sum_{i=1}^{N}\sum_{h=a,c}\frac{\wp_{hi,1}}{2}(\tilde{W}_{hi,1}^{\mathrm{T}}S_{Ri,1})^2-\\&\sum_{i=1}^{N}\frac{\wp_{ci,1}}{2}(\hat{W}_{ci,1}^{\mathrm{T}}S_{Ri,1})^2-\sum_{i=1}^{N}\left(\frac{\wp_{ai,1}}{2}-\frac{1}{4}\right)(\hat{W}_{ai,1}^{\mathrm{T}}S_{Ri,1})^2=\\&-\varDelta_{i,1}V_{i,1}+\Gamma_{i,1}+\sum_{i=1}^{N}\frac{\vartheta_{i,1}^2}{2}e_{i,2}^2\end{aligned} \tag{66}$$

where $\varDelta_{i,1}=\min\left\{\left(\tau_{i,1}-\frac{1}{2}\right),\wp_{fi,1}\rho_{fi,1},\wp_{ci,1}\right\}$ and $\Gamma_{i,1}=\sum_{i=1}^{N}\left(\psi_{i,1}^2\phi_{i,1}^2+\frac{1}{2}\wp_{ai,1}(W_{ai,1}^{\mathrm{T}}S_{Ri,1})^2+\frac{1}{2}\wp_{ci,1}(W_{ci,1}^{\mathrm{T}}S_{Ri,1})^2\right)-\frac{\rho_{fi,1}}{2}\rho_{fi,1}(\hat{W}_{fi,1}^{\mathrm{T}}\hat{W}_{fi,1}-W_{fi,1}^{\mathrm{T}}W_{fi,1})$.

Step *p* Choose the Lyapunov function as

$$V_{i,p}=\sum_{i=1}^{N}\left(\frac{1}{2}\varrho_{i,p}^2+\frac{1}{2\wp_{fi,p}}\tilde{W}_{fi,p}^{\mathrm{T}}\tilde{W}_{fi,p}+\frac{1}{2}\sum_{h=a,c}\tilde{W}_{hi,p}^{\mathrm{T}}\tilde{W}_{hi,p}\right) \tag{67}$$

where $\tilde{W}(\cdot)=\hat{W}(\cdot)-W(\cdot)$, and since $W(\cdot)$ is a constant, it follows that $\dot{\tilde{W}}(\cdot)=\dot{\hat{W}}(\cdot)$.

Similar to $V_{i,1}$, the derivative of $V_{i,p}$ can be expressed by the following expression

$$\begin{aligned}\dot{V}_{i,p}=&\sum_{i=1}^{N}\varrho_{i,p}(\psi_{i,p}(x_{i,p+1}+f_{i,p}(\bar{x}_{i,p})-\dot{\alpha}_{i,p-1}-\varpi_{i,p}\psi_{i,p}^{-1}))+\\&\sum_{i=1}^{N}\left\{\frac{1}{\wp_{fi,p}}\tilde{W}_{fi,p}^{\mathrm{T}}\wp_{fi,p}(\psi_{i,p}S_{fi,p}\varrho_{i,p}-\rho_{fi,p}\hat{W}_{fi,p})\right\}-\\&\sum_{i=1}^{N}\{\tilde{W}_{ai,p}^{\mathrm{T}}S_{Ri,p}S_{Ri,p}^{\mathrm{T}}(\wp_{ai,p}(\hat{W}_{ai,p}-\hat{W}_{ci,p})+\wp_{ci,p}\hat{W}_{ci,p})\}-\\&\sum_{i=1}^{N}\{\wp_{ci,p}\tilde{W}_{ci,p}S_{Ri,p}S_{Ri,p}^{\mathrm{T}}\hat{W}_{ci,p}\}\end{aligned} \tag{68}$$

Applying the Young's inequality, we have

$$\begin{aligned}&\sum_{i=1}^{N}\zeta_{i,p}e_{i,p+1}\leqslant\sum_{i=1}^{N}\frac{\varrho_{i,p}^2}{2}+\sum_{i=1}^{N}\frac{\psi_{i,p}^2e_{i,p+1}^2}{2},\\&\sum_{i=1}^{N}\wp_{ci,p}\tilde{W}_{ai,p}^{\mathrm{T}}S_{Ri,p}S_{Ri,p}^{\mathrm{T}}\hat{W}_{ci,p}\leqslant\sum_{i=1}^{N}\frac{\wp_{ci,p}(\tilde{W}_{ai,p}^{\mathrm{T}}S_{Ri,p})^2}{2}+\\&\sum_{i=1}^{N}\frac{\wp_{ci,p}(\hat{W}_{ci,p}S_{Ri,p}^{\mathrm{T}})^2}{2},\\&\sum_{i=1}^{N}\left(-\frac{1}{2\vartheta_{i,p}}\zeta_{i,p}\hat{W}_{ai,p}^{\mathrm{T}}S_{Ri,p}\right)\leqslant\sum_{i=1}^{N}\frac{\varrho_{i,p}^2}{4}+\sum_{i=1}^{N}\frac{(\hat{W}_{ai,p}^{\mathrm{T}}S_{Ri,p})^2}{4}\end{aligned} \tag{69}$$

where $\zeta_{i,p}=\varrho_{i,p}\psi_{i,p}$.

The organization of all previous reasoning results yields

$$\begin{aligned}\dot{V}_{i,p} \leqslant& \sum_{i=p}^{N}\frac{\vartheta_{i,p}^2}{2}e_{i,p+1}^2-\sum_{i=1}^{N}\left(\tau_{i,p}-\frac{3}{4}\right)\varrho_{i,p}^2+\Gamma_{i,p}-\\ &\sum_{i=1}^{N}\frac{\rho_{fi,p}}{2}W_{fi,p}^{\mathrm{T}}W_{fi,p}-\sum_{i=1}^{N}\sum_{h=a,c}\frac{\wp_{hi,p}}{2}(\tilde{W}_{hi,p}^{\mathrm{T}}S_{Ri,p})^2-\\ &\sum_{i=1}^{N}\frac{\wp_{ci,p}}{2}(\hat{W}_{ci,p}^{\mathrm{T}}S_{Ri,p})^2-\sum_{i=1}^{N}\left(\frac{\wp_{ai,p}}{2}-\frac{1}{4}\right)(\hat{W}_{ai,p}^{\mathrm{T}}S_{Ri,p})^2\end{aligned} \tag{70}$$

where $\varDelta_{i,p}=\min\left\{\left(2\tau_{i,p}-\frac{3}{2}\right),\wp_{fi,p}\rho_{fi,p},\wp_{ci,p}\right\}$ and $\Gamma_{i,p}=\sum_{i=1}^{N}\left(\psi_{i,p}^2\phi_{i,p}^2+\frac{1}{2}\wp_{ai,p}(W_{ai,p}^{\mathrm{T}}S_{Ri,p})^2+\frac{1}{2}\wp_{ci,p}(W_{ci,p}^{\mathrm{T}}S_{Ri,p})^2\right)-\frac{\rho_{fi,p}}{2}\rho_{fi,p}(\hat{W}_{fi,p}^{\mathrm{T}}\hat{W}_{fi,p}-W_{fi,p}^{\mathrm{T}}W_{fi,p})$.

Step *n* Choose the Lyapunov function as

$$\begin{aligned}V_{i,n}=&\sum_{i=1}^{N}\left(\frac{1}{2}\varrho_{i,n}^2+\frac{1}{2\wp_{fi,n}}\tilde{W}_{fi,n}^{\mathrm{T}}\tilde{W}_{fi,n}+\right.\\ &\left.\frac{1}{2}\sum_{h=a,c}\tilde{W}_{hi,n}^{\mathrm{T}}\tilde{W}_{hi,n}\right)\end{aligned} \tag{71}$$

where $\tilde{W}(\cdot)=\hat{W}(\cdot)-W(\cdot)$, and since $W(\cdot)$ is a constant, it follows that $\dot{\tilde{W}}(\cdot)=\dot{\hat{W}}(\cdot)$.

Similar to $V_{i,1}$ and $V_{i,p}$, the derivative of $V_{i,n}$ is

$$\begin{aligned}\dot{V}_{i,n}=&\sum_{i=1}^{N}\varrho_{i,n}[\psi_{i,n}(u_{i,n}+f_{i,n}(\bar{x}_{i,n})-\dot{\alpha}_{i,n-1}-\varpi_{i,n}\psi_{i,n}^{-1})]+\\ &\sum_{i=1}^{N}\left\{\frac{1}{\wp_{fi,n}}\tilde{W}_{fi,n}^{\mathrm{T}}\wp_{fi,n}(\psi_{i,n}S_{fi,n}\varrho_{i,n}-\rho_{fi,n}\hat{W}_{fi,n})\right\}-\\ &\sum_{i=1}^{N}\{\tilde{W}_{ai,n}^{\mathrm{T}}S_{Ri,n}S_{Ri,n}^{\mathrm{T}}[\wp_{ai,n}(\hat{W}_{ai,n}-\hat{W}_{ci,n})+\wp_{ci,n}\hat{W}_{ci,n}]\}-\\ &\sum_{i=1}^{N}\{\wp_{ci,n}\tilde{W}_{ci,n}S_{Ri,n}S_{Ri,n}^{\mathrm{T}}\hat{W}_{ci,n}\}\end{aligned} \tag{72}$$

Applying the Young's inequality, we have

$$\begin{aligned}&\sum_{i=1}^{N}\zeta_{i,n}e_{i,n}\leqslant\sum_{i=1}^{N}\frac{\varrho_{i,n}^2}{2}+\sum_{i=1}^{N}\frac{\psi_{i,p}^2e_{i,n}^2}{2},\\ &\sum_{i=1}^{N}\wp_{ci,n}\tilde{W}_{ai,n}^{\mathrm{T}}S_{Ri,n}S_{Ri,n}^{\mathrm{T}}\hat{W}_{ci,n}\leqslant\sum_{i=1}^{N}\frac{\wp_{ci,n}(\tilde{W}_{ai,n}^{\mathrm{T}}S_{Ri,n})^2}{2}+\\ &\sum_{i=1}^{N}\frac{\wp_{ci,n}(\hat{W}_{ci,n}S_{Ri,n}^{\mathrm{T}})^2}{2},\\ &\sum_{i=1}^{N}\left(-\frac{1}{2\vartheta_{i,n}}\zeta_{i,n}\hat{W}_{ai,n}^{\mathrm{T}}S_{Ri,n}\right)\leqslant\sum_{i=1}^{N}\frac{\varrho_{i,n}^2}{4}+\sum_{i=1}^{N}\frac{(\hat{W}_{ai,p}^{\mathrm{T}}S_{Ri,n})^2}{4}\end{aligned} \tag{73}$$

where $\zeta_{i,n}=\varrho_{i,n}\psi_{i,n}$.

Combining all the formulas from $v_{i,1}$ to $v_{i,n}$ yields

$$\begin{aligned}\dot{V}_{i,n}\leqslant&\sum_{i=n}^{N}\frac{\vartheta_{i,n}^2}{2}e_{i,n}^2-\sum_{i=1}^{N}\left(\tau_{i,n}-\frac{3}{4}\right)\varrho_{i,n}^2+\Gamma_{i,n}-\\ &\sum_{i=1}^{N}\frac{\rho_{fi,n}}{2}W_{fi,n}^{\mathrm{T}}W_{fi,n}-\sum_{i=1}^{N}\sum_{h=a,c}\frac{\wp_{hi,n}}{2}(\tilde{W}_{hi,n}^{\mathrm{T}}S_{Ri,n})^2-\\ &\sum_{i=1}^{N}\frac{\wp_{ci,n}}{2}(\hat{W}_{ci,n}^{\mathrm{T}}S_{Ri,n})^2-\sum_{i=1}^{N}\left(\frac{\wp_{ai,n}}{2}-\frac{1}{4}\right)(\hat{W}_{ai,n}^{\mathrm{T}}S_{Ri,n})^2\end{aligned} \tag{74}$$

where $\varDelta_{i,n}=\min\left\{\left(2\tau_{i,n}-\frac{3}{2}\right),\wp_{fi,n}\rho_{fi,n},\wp_{ci,n}\right\}$ and $\Gamma_{i,n}=\sum_{i=1}^{N}\left(\psi_{i,n}^2\phi_{i,n}^2+\frac{1}{2}\wp_{ai,n}(W_{ai,n}^{\mathrm{T}}S_{Ri,n})^2+\frac{1}{2}\wp_{ci,n}(W_{ci,n}^{\mathrm{T}}S_{Ri,n})^2\right)-\frac{\rho_{fi,n}}{2}\rho_{fi,n}(\hat{W}_{fi,n}^{\mathrm{T}}\hat{W}_{fi,n}-W_{fi,n}^{\mathrm{T}}W_{fi,n})$.

Finally, select $V=V_{i,1}+V_{i,2}+\cdots+V_{i,n}=\sum_{q=1}^{n}V_{i,q}$ to serve as a Lyapunov function candidate. The derivative of V is obtained by combining Eqs. (67), (71), and (75), resulting in the following expression

$$\begin{aligned}V=&\sum_{i=1}^{N}\sum_{q=1}^{n}\left[\frac{1}{2}\varrho_{i,q}^2+\frac{1}{2\wp_{fi,q}}\tilde{W}_{fi,q}^{\mathrm{T}}\tilde{W}_{fi,q}+\frac{1}{2}\sum_{h=a,c}\tilde{W}_{hi,q}^{\mathrm{T}}\tilde{W}_{hi,q}\right]\leqslant\\ &-\varDelta V+\Gamma\end{aligned} \tag{75}$$

where $\varDelta=\min\{\varDelta_{i,q}\}$, $\Gamma=\sum_{q=1}^{n}\Gamma_{i,q}$, and $q=1,2,\ldots,n$. ■

Combining the properties of V with the above derivation, it is not difficult to conclude that variables $\tilde{W}_{ai,q}$, $\tilde{W}_{fi,q}$, and $\tilde{W}_{ci,q}$ for $q=1,2,\ldots,n$ are semi-globally uniformly ultimately bounded, so that the consensus tracking error $\varrho_{i,q}$ for $q=1,2,\ldots,n$ is bounded. Therefore, by utilizing the Lyapunov function and the ETF mentioned above, the bipartite consensus error will converge within a fixed time and meet the prescribed performance control objectives.

V. SIMULATIONS

In this section, numerical simulations via MATLAB are conducted to validate the effectiveness of the proposed control protocol. The MASs are considered to be moving in a two-dimensional plane, which consists of 3 followers and 1 leader. The topological communication diagram is shown in Fig. 1. The dynamics of each follower can be described by the following equations

$$\begin{cases}\dot{x}_{i,1}=x_{i,2}+f_{i,1}(\bar{x}_{i,1}),\\ \dot{x}_{i,2}=u_i+f_{i,2}(\bar{x}_{i,2}),\\ y_i=x_{i,1}\end{cases} \tag{76}$$

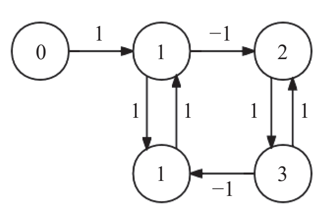

Fig. 1 Communication topology.

Since there are four followers, i takes the values 1, 2, 3, and 4. The state vectors are denoted as $x_{i,1}=[x_{i,1X},x_{i,1Y}]^{\mathrm{T}}$ and $x_{i,2}=[x_{i,2X},x_{i,2Y}]^{\mathrm{T}}$, the control input vector is denoted as $u_i=[u_{i,X}, u_{i,Y}]^{\mathrm{T}}$, and the output vector is denoted as $y_i=[y_{i,X},y_{i,Y}]^{\mathrm{T}}$. Although agent i for $i=1,2,3,4$ has the same control structure, each agent possesses a nonlinear function of different forms as

$$\begin{aligned}
&f_{1,1}(\cdot)=[0.01\sin(x_{1,1X}),0.01\sin(x_{1,1Y})]^{\mathrm{T}},\\
&f_{2,1}(\cdot)=[0.01\sin(x_{2,1X}),0.01\sin(x_{2,1Y})]^{\mathrm{T}},\\
&f_{3,1}(\cdot)=[0.01\sin(x_{3,1X}),0.01\sin(x_{3,1Y})]^{\mathrm{T}},\\
&f_{1,2}(\cdot)=[0.01\sin(x_{1,1X}x_{1,2X}),0.01\sin(x_{1,1Y}x_{1,2Y})]^{\mathrm{T}},\\
&f_{2,2}(\cdot)=[0.01\sin(x_{2,1X}x_{2,2X}),0.01\sin(x_{2,1Y}x_{2,2Y})]^{\mathrm{T}},\\
&f_{3,2}(\cdot)=[0.01\sin(x_{3,1X}x_{3,2X}),0.01\sin(x_{3,1Y}x_{3,2Y})]^{\mathrm{T}}
\end{aligned}\tag{77}$$

The initial states of the four followers are chosen as

$$\begin{aligned}
&x_{1,1}(0)=[0.010,1.110]^{\mathrm{T}},\\
&x_{2,1}(0)=[0.011,1.111]^{\mathrm{T}},\\
&x_{3,1}(0)=[0.012,0.110]^{\mathrm{T}}
\end{aligned}\tag{78}$$

In the design of the optimal controller, all FLSs include 6 membership functions. The values of p_i and η_i for the Gaussian function are both set to 2. The parameter l in the quantizer is set to a value of 0.02. Additionally, for the initial weight values in the x-direction, they are taken as $W_{fi,1_X}(0)=[0.1,0.1,\ldots,0.1]^{\mathrm{T}}\in\mathbb{R}^{6\times1}$, $W_{fi,2_X}(0)=[0.5,0.5,\ldots,0.5]^{\mathrm{T}}\in\mathbb{R}^{6\times1}$, $W_{ai,1_X}(0)=[0.2,0.2,\ldots,0.2]^{\mathrm{T}}\in\mathbb{R}^{6\times1}$, $W_{ai,2_X}(0)=[0.3,0.3,\ldots,0.3]^{\mathrm{T}}\in\mathbb{R}^{6\times1}$, $W_{ci,1_X}(0)=[0.2,0.2,\ldots,0.2]^{\mathrm{T}}\in\mathbb{R}^{6\times1}$, and $W_{ci,2_X}(0)=[0.3,0.3,\ldots,0.3]^{\mathrm{T}}\in\mathbb{R}^{6\times1}$. For the initial weight values in the y-direction, they are established as $W_{fi,1_Y}(0)=[0.3,0.3,\ldots,0.3]^{\mathrm{T}}\in\mathbb{R}^{6\times1}$, $W_{fi,2_Y}(0)=[0.5,0.5,\ldots,0.5]^{\mathrm{T}}\in\mathbb{R}^{6\times1}$, $W_{ai,1_Y}(0)=[0.6,0.6,\ldots,0.6]^{\mathrm{T}}\in\mathbb{R}^{6\times1}$, $W_{ai,2_Y}(0)=[0.3,0.3,\ldots,0.3]^{\mathrm{T}}\in\mathbb{R}^{6\times1}$, $W_{ci,1_Y}(0)=[0.6,0.6,\ldots,0.6]^{\mathrm{T}}\in\mathbb{R}^{6\times1}$, and $W_{ci,2_Y}(0)=[0.3,0.3,\ldots,0.3]^{\mathrm{T}}\in\mathbb{R}^{6\times1}$.

The parameter settings related to the FTPPF in the x-direction are as follows: $\kappa_{1,1_X}=\kappa_{2,1_X}=\kappa_{3,1_X}=\kappa_{4,1_X}=1$, $o_{1,1_X}=o_{2,1_X}=o_{3,1_X}=o_{4,1_X}=2$, $\delta_{1,1_X}=\delta_{2,1_X}=\delta_{3,1_X}=\delta_{4,1_X}=1$, $\nu_{1,1,0_X}=\nu_{2,1,0_X}=\nu_{3,1,0_X}=\nu_{4,1,0_X}=1.2$, and $\nu_{\tilde{\Upsilon}_{1,1_X}}=\nu_{\tilde{\Upsilon}_{2,1_X}}=\nu_{\tilde{\Upsilon}_{3,1_X}}=\nu_{\tilde{\Upsilon}_{4,1_X}}=0.1$. The parameter settings related to the FTPPF in the y-direction are as follows: $\kappa_{1,1_Y}=\kappa_{2,1_Y}=\kappa_{3,1_Y}=\kappa_{4,1_Y}=1$, $o_{1,1_Y}=o_{2,1_Y}=o_{3,1_Y}=o_{4,1_Y}=2$, $\delta_{1,1_Y}=\delta_{2,1_Y}=\delta_{3,1_Y}=\delta_{4,1_Y}=1$, $\nu_{1,1,0_Y}=\nu_{2,1,0_Y}=\nu_{3,1,0_Y}=\nu_{4,1,0_Y}=1.2$, and $\nu_{\tilde{\Upsilon}_{1,1_Y}}=\nu_{\tilde{\Upsilon}_{2,1_Y}}=\nu_{\tilde{\Upsilon}_{3,1_Y}}=\nu_{\tilde{\Upsilon}_{4,1_Y}}=0.1$.

The weight adaptive updating parameters in the x-direction are set to $\wp_{fi,1_X}=0.01$, $\rho_{fi,1_X}=100$, $\wp_{ai,1_X}=40$, $\wp_{ci,1_X}=40$, $\wp_{fi,2_X}=0.8$, $\rho_{fi,2_X}=5$, $\wp_{ai,2_X}=30$, and $\wp_{ci,2_X}=30$. The weight adaptive updating parameters in the y-direction are set to $\wp_{fi,1_Y}=0.01$, $\rho_{fi,1_Y}=200$, $\wp_{ai,1_Y}=30$, $\wp_{ci,1_Y}=30$, $\wp_{fi,2_Y}=0.1$, $\rho_{fi,2_Y}=20$, $\wp_{ai,2_Y}=80$, and $\wp_{ci,2_Y}=80$.

Simulation verification is conducted via MATLAB, and the results are shown in Figs. 2–8. Fig. 2 illustrates the comparison between the quantized signal y_q and the original signal y_r, demonstrating that even if the signal transmission loses its

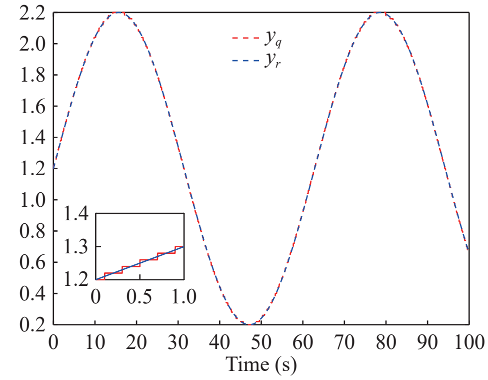

Fig. 2 The quantized signal y_q and the original signal y_r.

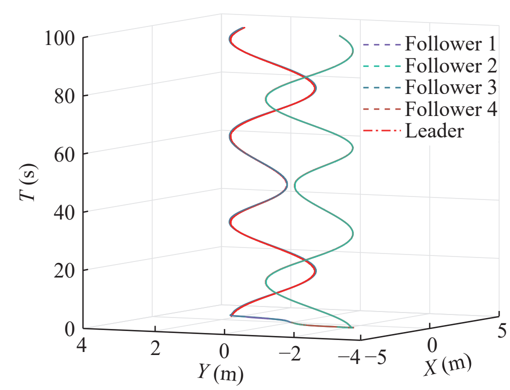

Fig. 3 The two-dimensional paths of the leader and four followers.

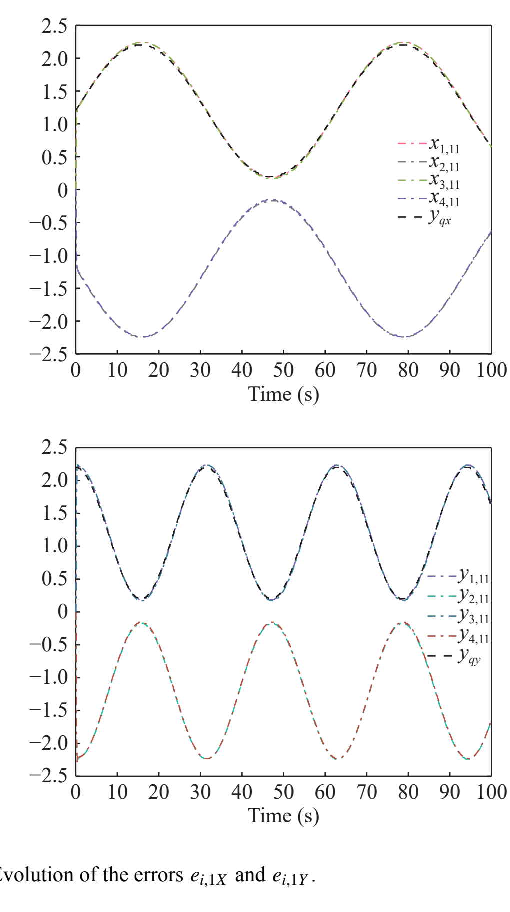

Fig. 4 Evolution of the errors $e_{i,1X}$ and $e_{i,1Y}$.

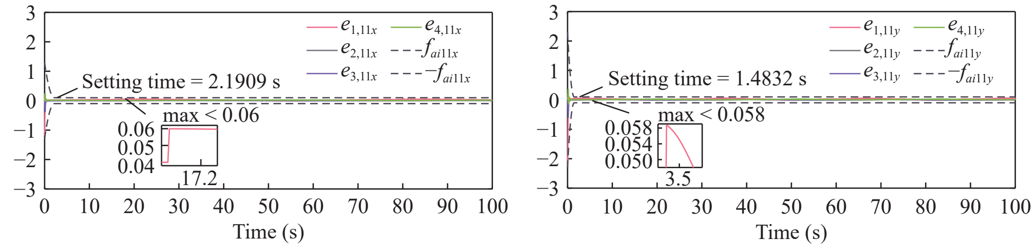

Fig. 5 Performance of the bipartite control in the x-direction and y-direction.

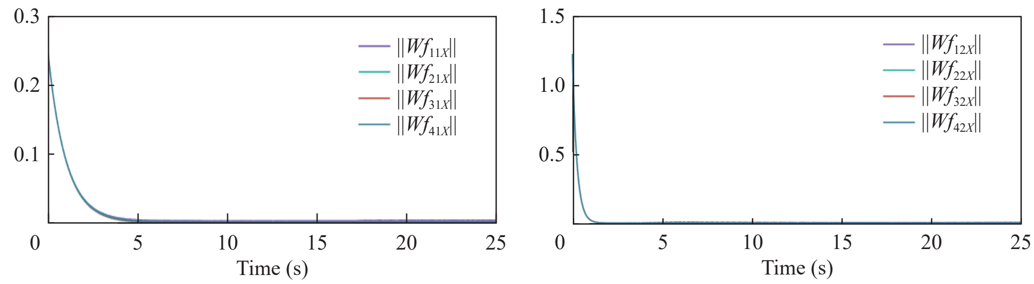

Fig. 6 The identifier FLS weight norms in the x-direction.

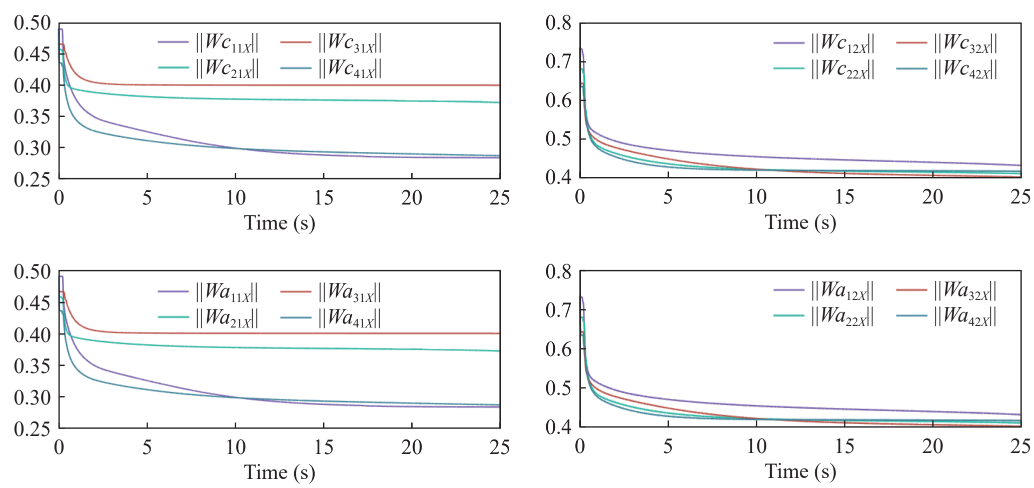

Fig. 7 The critic FLS weight norms and actor FLS weight norms in the x-direction.

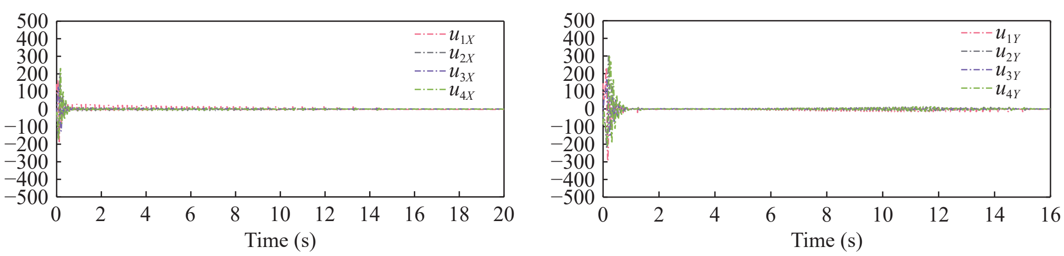

Fig. 8 The control input signals of u_x and u_y.

exact value at a certain moment, it can still communicate values that are very close to the true values. Figs. 3 and 4 show that the four followers can successfully track the motion trajectory of the leader and engage in coordinated motion. Moreover, Fig. 5 clearly illustrates that the errors $e_{i,1X}$ and $e_{i,1Y}$ of the four followers in the x-direction and y-direction accurately converge to the predefined performance bounds within a specified time frame. The maximum values in the x-direction and y-direction are observed to be < 0.060 and < 0.059 after stabilization, thereby ensuring that the preset performance requirements are satisfied. The evolution of the norms of the identifier, critic, and actor in the x-direction is successively depicted in Figs. 6 and 7, which demonstrate the convergence of the adaptive law designed in this paper. Fig. 8

demonstrates that the controller designed in this paper is effective.

VI. Conclusion

This paper addresses the issue of bipartite output consensus tracking for nonlinear coopetition MASs with the leader's reference signal being quantized by proposing an FTPPF. Within this control protocol, FLSs are utilized to approximate the unknown nonlinear dynamics that arise in the design of the virtual controller, and an RL framework based on the ICA structure is integrated. Ultimately, through simulation experiments, it is demonstrated that the errors successfully converge within a fixed time to the pre-specified interval, achieving the desired control requirements and ensuring the effectiveness of the proposed method.

Acknowledgment

This work was supported by the National Natural Science Foundation of China (No. 62322307) and the Sichuan Science and Technology Program (No. 2023NSFSC1968).

References

[1] X. Min, S. Baldi, and W. Yu, Distributed output feedback funnel control for uncertain nonlinear multiagent systems, *IEEE Trans. Fuzzy Syst.*, 2022, 30(9), 3708–3721.

[2] Z. Lin and F. Xu, Simulation of robot automatic control model based on artificial intelligence algorithm, in *Proc. 2023 2nd International Conference on Artificial Intelligence and Autonomous Robot Systems*, Bristol, UK, 2023, 535–539.

[3] H. Sánchez San Blas, A. Filipe Sales Mendes, F. Pérez Robledo, G. Villarrubia González, and J. F. de Paz Santana, A multi-agent system approach for balance disorder treatment: Integrating computer vision and gamification, *IEEE Access*, 2024, 12, 118649–118664.

[4] H. Zhou and S. Tong, Fuzzy adaptive resilient formation control for nonlinear multiagent systems subject to DoS attacks, *IEEE Trans. Fuzzy Syst.*, 2024, 32(3), 1446–1454.

[5] J. Qin, Q. Ma, P. Yi, and L. Wang, Multiagent interval consensus with flocking dynamics, *IEEE Trans. Autom. Control*, 2022, 67(8), 3965–3980.

[6] J. Gabriel and J. Deutscher, Robust cooperative output regulation for networks of hyperbolic PIDE-ODE systems, *IEEE Trans. Autom. Control*, 2024, 69(2), 888–903.

[7] F. M. Zegers, P. Deptula, J. M. Shea, and W. E. Dixon, Event-triggered approximate leader-follower consensus with resilience to byzantine adversaries, in *Proc. 2019 IEEE 58th Conference on Decision and Control*, Nice, France, 2019, 6412–6417.

[8] Z. Li and J. Zhao, Adaptive consensus of non-strict feedback switched multi-agent systems with input saturations, *IEEE/CAA J. Autom. Sin.*, 2021, 8(11), 1752–1761.

[9] J. Wang, G. Wen, and Z. Duan, Distributed antiwindup consensus control of heterogeneous multiagent systems over Markovian randomly switching topologies, *IEEE Trans. Autom. Control*, 2022, 67(11), 6310–6317.

[10] Y. Liu, X. Xie, R. M. Palhares, and J. Sun, DMET-based fuzzy optimized consensus control for nonlinear MASs with quantized reference, *IEEE Trans. Fuzzy Syst.*, 2024, 32(6), 3556–3567.

[11] H. Zhang, Q. Wei, and Y. Luo, A novel infinite-time optimal tracking control scheme for a class of discrete-time nonlinear systems via the greedy HDP iteration algorithm, *IEEE Trans. Syst. Man Cybern. B Cybern.*, 2008, 38(4), 937–942.

[12] Q. Wang, Z. Duan, and J. Wang, Distributed optimal consensus control algorithm for continuous-time multi-agent systems, *IEEE Trans. Circuits Syst. II Express Briefs*, 2020, 67(1), 102–106.

[13] J. Yu, X. Dong, Q. Li, J. Lü, and Z. Ren, Adaptive practical optimal time-varying formation tracking control for disturbed high-order multi-agent systems, *IEEE Trans. Circuits Syst. I Regul. Pap.*, 2022, 69(6), 2567–2578.

[14] L. Yuan and J. Li, Consensus of discrete-time nonlinear multiagent systems using sliding mode control based on optimal control, *IEEE Access*, 2022, 10, 47275–47283.

[15] H. Li and Q. Wei, Data-driven optimal output cluster synchronization control of heterogeneous multi-agent systems, *IEEE Trans. Autom. Sci. Eng.*, 2024, 21(3), 3910–3920.

[16] Y. Ren, Q. Wang, and Z. Duan, Optimal distributed leader-following consensus of linear multi-agent systems: A dynamic average consensus-based approach, *IEEE Trans. Circuits Syst. II Express Briefs*, 2022, 69(3), 1208–1212.

[17] L. Zhang and Y. Chen, Distributed finite-time ADP-based optimal control for nonlinear multiagent systems, *IEEE Trans. Circuits Syst. II Express Briefs*, 2023, 70(12), 4534–4538.

[18] H. Zhang, H. Jiang, Y. Luo, and G. Xiao, Data-driven optimal consensus control for discrete-time multi-agent systems with unknown dynamics using reinforcement learning method, *IEEE Trans. Ind. Electron.*, 2017, 64(5), 4091–4100.

[19] G. Wen and C. Chen, Optimized backstepping consensus control using reinforcement learning for a class of nonlinear strict-feedback-dynamic multi-agent systems, *IEEE Trans. Neural Networks Learn. Syst.*, 2023, 34(3), 1524–1536.

[20] B. Xu, Y.-X. Li, Z. Hou, and C. K. Ahn, Dynamic event-triggered reinforcement learning-based consensus tracking of nonlinear multi-agent systems, *IEEE Trans. Circuits Syst. I Regul. Pap.*, 2023, 70(5), 2120–2132.

[21] X. Yue, H. Zhang, J. Sun, T. Wang, and L. Liu, Optimized backstepping-based containment control for multiagent systems with deferred constraints using a universal nonlinear transformation, *IEEE Trans. Cybern.*, 2024, 54(10), 6058–6068.

[22] Y. Cai, H. Zhang, Z. Gao, L. Yang, and Q. He, Adaptive bipartite event-triggered time-varying output formation tracking of heterogeneous linear multi-agent systems under signed directed graph, *IEEE Trans. Neural Networks Learn. Syst.*, 2023, 34(10), 7049–7058.

[23] J. Liang, X. Bu, L. Cui, and Z. Hou, Data-driven bipartite formation for a class of nonlinear MIMO multiagent systems, *IEEE Trans. Neural Networks Learn. Syst.*, 2023, 34(6), 3161–3173.

[24] D. Yue, C. Deng, C. Wen, and W. Wang, Finite-time distributed resilient tracking control for nonlinear mass with application to power systems, *IEEE Trans. Autom. Control*, 2024, 69(5), 3128–3143.

[25] H. Liang, L. Chen, Y. Pan, and H. K. Lam, Fuzzy-based robust precision consensus tracking for uncertain networked systems with cooperative-antagonistic interactions, *IEEE Trans. Fuzzy Syst.*, 2023, 31(4), 1362–1376.

[26] M. Sader, W. Li, H. Jiang, Z. Chen, and Z. Liu, Semi-global bipartite fault-tolerant containment control for heterogeneous multiagent systems with antagonistic communication networks and input saturation, *IEEE Trans. Neural Networks Learn. Syst.*, 2024, 35(5), 6265–6272.

[27] F. Sedghi, M. M. Arefi, A. Abooee, and S. Yin, Distributed adaptive-neural finite-time consensus control for stochastic nonlinear multiagent

systems subject to saturated inputs, *IEEE Trans. Neural Networks Learn. Syst.*, 2023, 34(10), 7704–7718.

[28] C. Huang, Z. Liu, C. Chen, and Y. Zhang, Adaptive fixed-time neural control for uncertain nonlinear multiagent systems, *IEEE Trans. Neural Networks Learn. Syst.*, 2023, 34(12), 10346–10358.

[29] L. Zhang, B. Chen, C. Lin, and Y. Shang, Fuzzy adaptive fixed-time consensus tracking control of high-order multiagent systems, *IEEE Trans. Fuzzy Syst.*, 2022, 30(2), 567–578.

[30] W. Bi, C. Zhang, S. Sui, S. Tong, and C. Chen, Fixed-time fuzzy adaptive bipartite output consensus tracking for nonlinear coopetition MASs, *IEEE Trans. Fuzzy Syst.*, 2024, 32(5), 2775–2785.

[31] Z. Zhang and Z. Chen, Consensus of discrete-time multiagent systems with transient performance constraints, *IEEE Trans. Autom. Control*, 2024, 69(10), 7096–7103.

[32] S. Luo, Y. Song, F. L. Lewis, and G. Deng, Dynamical analysis, circuit design, and fuzzy prescribed performance backstepping control of the FO weakly coupled MEMS resonators, *IEEE Trans. Fuzzy Syst.*, 2024, 32(4), 1768–1781.

[33] L. Zhang, W.-W. Che, C. Deng, and Z.-G. Wu, Prescribed performance control for multiagent systems via fuzzy adaptive event-triggered strategy, *IEEE Trans. Fuzzy Syst.*, 2022, 30(12), 5078–5090.

[34] H. Zhou, S. Sui, and S. Tong, Finite-time adaptive fuzzy prescribed performance formation control for high-order nonlinear multiagent systems based on event-triggered mechanism, *IEEE Trans. Fuzzy Syst.*, 2023, 31(4), 1229–1239.

[35] S. Huang, G. Zong, B. Niu, N. Xu, and X. Zhao, Dynamic self-triggered fuzzy bipartite time-varying formation tracking for nonlinear multiagent systems with deferred asymmetric output constraints, *IEEE Trans. Fuzzy Syst.*, 2024, 32(5), 2700–2712.

[36] Y. Cai, H. Zhang, Y. Wang, Z. Gao, and Q. He, Adaptive bipartite fixed-time time-varying output formation-containment tracking of heterogeneous linear multiagent systems, *IEEE Trans. Neural Networks Learn. Syst.*, 2022, 33(9), 4688–4698.

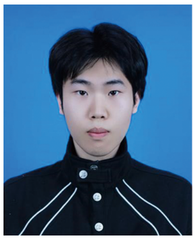

Jiaming Guo received the BS degree in marine engineering from Dalian Maritime University, Dalian, China, in 2023. He is currently a graduate researcher in control science and engineering at School of Automation Engineering, University of Electronic Science and Technology of China, Chengdu, China, and also at Laboratory of Electromagnetic Space Cognition and Intelligent Control, University of Electronic Science and Technology of China, Chengdu, China. His research interests include multi-agent systems and optimal control.

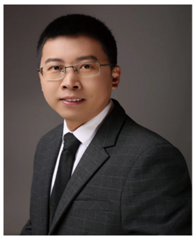

Hongjing Liang received the BS degree in mathematics from Bohai University, Jinzhou, China, in 2009, and the MS degree in fundamental mathematics and the PhD degree in control theory and control engineering from Northeastern University, Shenyang, China, in 2011 and 2016, respectively. He was a temporary research associate at Science Program, Texas A&M University, Doha, Qatar. He is currently a professor at University of Electronic Science and Technology of China, Chengdu, China. He was the recipient of the Outstanding Reviewer Award of CAA/Automatica Sinica 2019. He has been in the editorial board of *International Journal of Fuzzy Systems* and *Fluctuation and Noise Letters*. His research interests include adaptive control, fuzzy control, and cooperative control and their applications.

Chenhong An received the BS degree in automation engineering from University of Electronic Science and Technology of China, Chengdu, China, in 2023. He is currently a graduate researcher in control science and engineering at School of Automation Engineering, University of Electronic Science and Technology of China, Chengdu, China, and also at Laboratory of Electromagnetic Space Cognition and Intelligent Control, University of Electronic Science and Technology of China, Chengdu, China. His research interests include multi-agent systems and optimal control.